NON-LINEAR FINITE ELEMENT ANALYSIS OF RC BEAMS WITH SPECIAL DETAILING OF STIRRUPS

Mohammed Arafa* and Mohamed Ziara#

* Chairman and Assistant Professor, Department of Civil Engineering, IUG, P. O. Box 108, Gaza, Palestine. Tel: +972 8 2860700, fax: 2860800 E-mail: marafa@mail.iugaza.edu.

\# Associate Professor, Department of Civil Engineering, IUG (on leave from Birzeit University). Telfax: +972(0)8 2824413. E-mail: mziara@birzeit.edu.

1 ABSTRACT

The paper includes the development and application of a non-linear finite element model for studying the structural behavior of beams designed using a flexure-shear interaction model. A two-dimensional material model with elasto–plastic and quadratic hardening function is used for concrete. The model takes the influence of confinement due to stirrups into considerations. The cracks propagation is modeled using a rotating crack smeared model. A modified quadratic Lagrange isoparametric element is used for modeling the concrete. This modeling allows variable positions of the interior nodes on both the edge and within the element. A bilinear elasto–plastic model is used for steel. The effect of tension stiffening and tension softening is considered in the analysis. Each bar of the reinforcement is modeled using either a discrete or a smeared model. A quadratic one dimensional isoparametric element is used for steel. The flexure-shear interaction design model considers the influence of shear force on reducing the flexural capacity of beams. The full flexural capacity is achieved by providing the load path within the beam with confinement stirrups. The beneficial influence of confinement on the strength and ductility of concrete is utilized in preventing the brittle shear failure. The test results have confirmed the applicability of the developed non-linear finite element and the flexure-shear interaction models. There was a good matching between the test results and the finite element analysis.

2 INTRODUCTION

Normal size and short beams subjected to transverse loading may fail by diagonal cracking due to shear if they are not provided with web reinforcement. Traditional design methods for shear [1,2] are based on truss analogy developed by Mörsh one century ago [3]. These approaches do not necessary represent actual behavior of beams. They ignore the shear-flexure interaction behavior. The beam is first designed for flexure then checked for shear. The nominal (average) shear strength "$v = V/bd$" assumed to occur on a section perpendicular to the beam axis is not a real indicator for shear strength of the beam since failure occurs along diagonal surface due the development of tensile stresses. The applied shear is assumed to be resisted by the concrete shear strength through beam and/or arch actions while the remaining shear is resisted by shear reinforcement through a truss action. The assumption of simultaneous occurrence of three actions to resist applied shear is totally unrealistic since this would result in strain incompatibility. Recognizing these limitations, a more realistic approach for shear design "flexure-shear interaction design model" has been developed based on actual behavior of beams [4].

3 FLEXURE-SHEAR INTERACTION DESIGN MODEL

The developed flexure-shear interaction design model considers one mechanism only to resist applied transverse loads as shown in Fig. 1. The load is transmitted to the supports along a load path that consists of a horizontal part in the middle of the beam and two inclined parts near the supports. The horizontal part bends towards the supports starting from a distance equal to either "2d" (for type II normal size beams with a/d > 2) or "a" (for type III short beams with a/d ≤ 2). Diagonal failure of the beam occurs due to the development of tensile stresses transverse to the load path. In the developed model diagonal failure of the beam is prevented by providing this path with confining stirrups as shown in Fig. 1. The horizontal part of the path is provided with short stirrups that extend down to half the beam depth. The inclined part of the path is provided with traditional long stirrups in order to confine the entire path depth in this region.

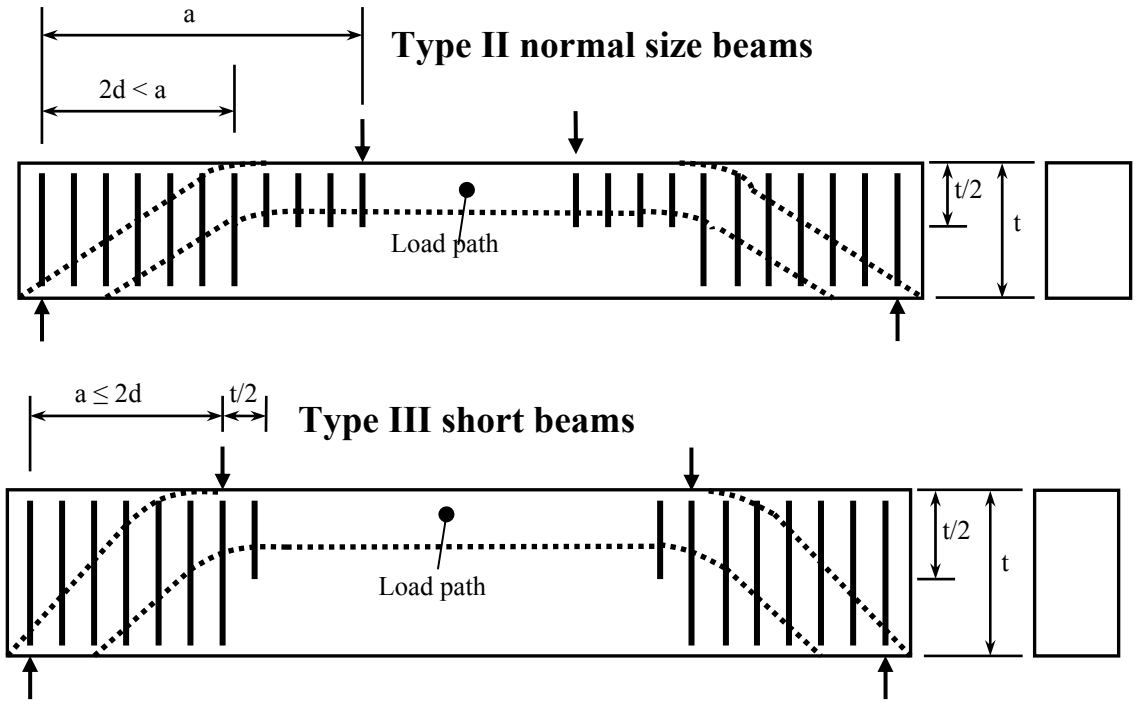

Fig. 1 Detailing based on the flexure-shear interaction design model.

The enhancement influence of the confinement stirrups on the strength and ductility of concrete prevents the development of tensile stresses from occurrence in all parts of the load path. Thus, the stirrups succeed in preventing the brittle diagonal failure in the beam. The amount of the confining stirrups is determined based on the interaction behavior between shear and flexure. It should be mentioned that the complete development of the analytical model and its practical verification have been already published [4,5]. This paper includes the application of a proposed non-linear finite element model for studying the behavior of test beams designed and detailed based on the flexure-shear interaction design model [6].

4 FINITE ELEMENT ANALYSIS

In numerical analysis based on finite elements, a structure is divided into a number of elements which are interconnected by nodes. The nodes are usually located at element

corner, element edges or may be inside the element. The results of the analysis are given at so-called integration points, which are located inside the element. A nonlinear analysis requires knowledge of several material parameter in additional to the modulus of elasticity "E" and Poisson's ratio "ν", which are normally needed in linear elastic analysis. The material model for concrete and steel used in the proposed nonlinear analysis is shortly described in the next subsections. It worthwhile mentioning that, using of discrete model for representing the main reinforcement, has the advantage of accurately representing different material properties. The discrete representation of reinforcement is the only direct way of accounting for bond slip and dowel action. The main disadvantage however, is that the finite element mesh patterns are restricted by the location of reinforcement. This means that the boundaries of the concrete elements have to follow the reinforcing bars, which would generate an irregular finite element meshes. In this model main reinforcing bars of arbitrary type and location are represented using a discrete model independent of the concrete finite element mesh. The problem of mesh dependency is overcome using Lagrange quadratic and cubic isoparametric elements with movable sides and interior nodes, which utilize a correction technique for node mapping distortion. No singular Jacobian matrix is obtained although the edge nodes are moved sufficiently from their normal positions [6,7,8]. The secondary reinforcement and stirrups are represented by a smeared model. The reinforcement bars are assumed to be uniformly distributed in the smeared model. A contact element with different bond conditions is used to model the bond behaviour between concrete and steel.

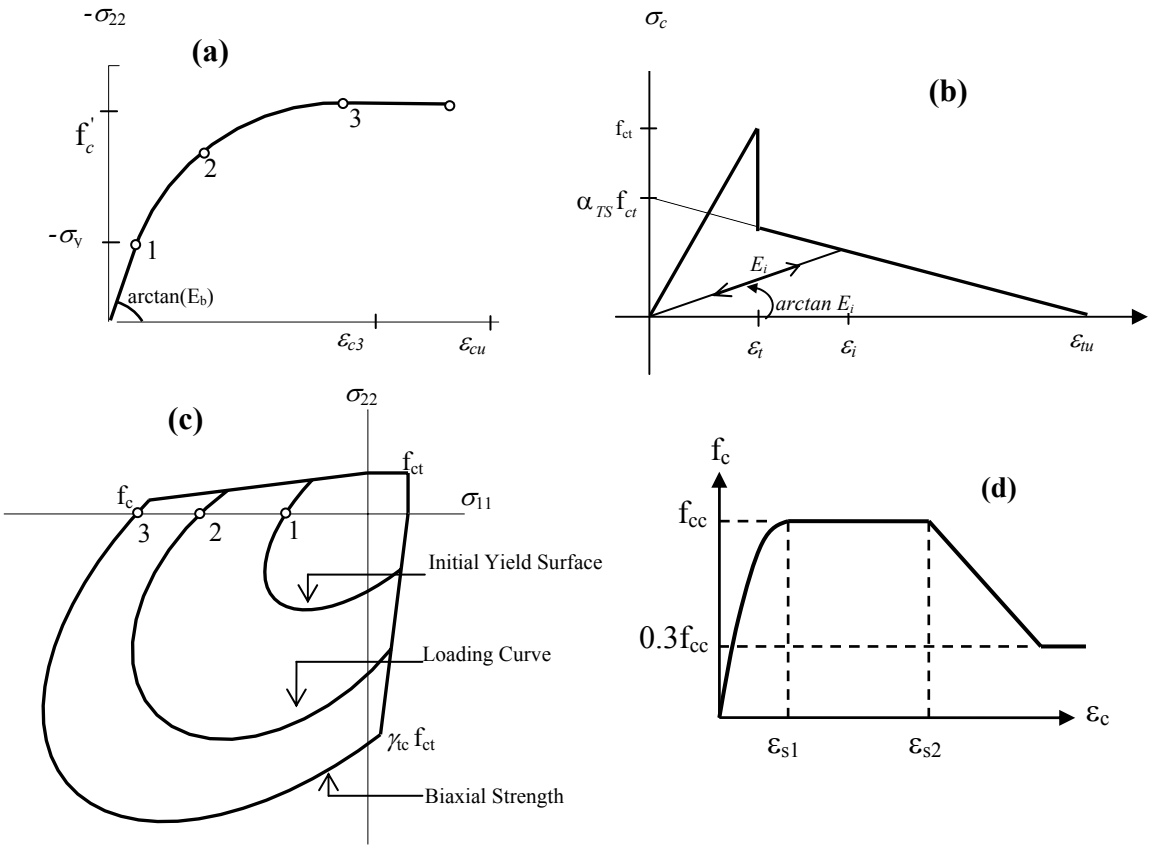

Fig.2 Uniaxial stress strain diagram under (a) compression and (b) tension; (c) Two dimension failure envelope and (d) Stress strain relationship for confined concrete.

4.1 Concret Material Model

An elasto-plastic concrete material model with quadratic hardening function shown in Fig. 2 (a,b and c) is used in the finite element analysis. This model was developed by Figueiras [9] and implemented by Dinges [10] and Kollegger [11] for the analysis of reinforced concrete shell structures. This model takes into account the rotating crack model, tension stiffening and softening effects. Prevention of shear failure based on the flexure-shear interaction model is achieved by utilizing the enhancement influence of the confinement stirrups on the strength (f_{cc}) and ductility (ε_c) of concrete. To allow for this influence the elasto-plastic concrete material model shown in Fig. 2 has been modified based on the confinement model by Sheikh [12]. The increase in concrete strength is calculated based on an effectively confined concrete area, which is less than the concrete core area enclosed by the centre line of the perimeter tie. The corresponding stress strain relationship is shown in Fig. 2.d [12].

4.2 Steel Material Model

A bilinear elasto-plastic material steel model shown in Fig. 3 is used in the finite element analysis [13]. In this model a linear elastic behavior until the yield point is used. After exceeding the yield stress a linear strain hardening is considered. Loading, unloading and reload are assumed to have the same initial modulus of elasticity.

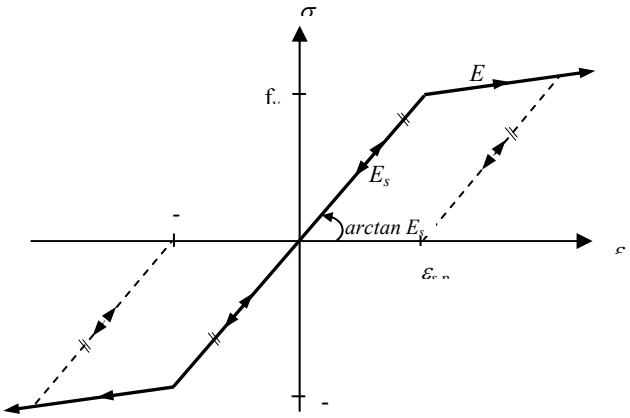

Fig. 3 Stress strain diagram for

4.3 Modelling of Concrete Cracking

The concrete cracking model includes the prediction of crack initiation, crack propagation and a method of crack representation. Initiation of cracking is usually determined by a strength criterion. The evolution of a crack is described by a criterion based on fracture mechanics [14]. Discrete or smeared crack models shown in Fig. 4 are normally used for representation of cracks. The discrete crack model was the first attempt to model cracking by introducing discrete cracks with a predetermined location and orientation [15]. This model was only applicable to problems with a few dominant cracks of priori known location and orientation. The main disadvantage of discrete

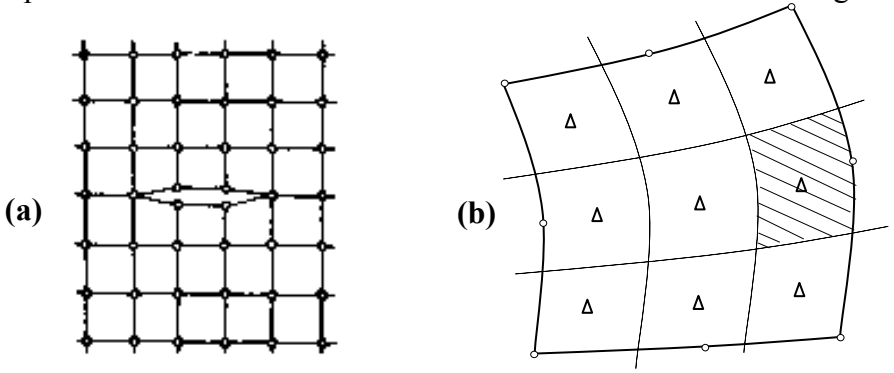

Fig. 4 Crack Model: (a) Discrete: b) Smeared at an integration point.

crack models is the large computational effort required for the introduction of new nodes or new DOF's and redefine the FE Mesh to model the crack propagations. In the smeared crack model the cracks are assumed to be smeared over the region associated with the integration points of finite element, a change of the FE-mesh is not required. The smeared crack models are suitable for the prediction of the global structural behavior. As soon as the main stresses at a concerned integration point exceed the tensile strength, the concrete at that point is considered as cracked concrete. The crack direction runs perpendicularly to the main stress. The cracking can either with fixed orthogonal crack, fixed non-orthogonal crack or rotating crack models [9,11,14]. In this paper, the smeared rotating crack model is adopted because this model is motivated by the experimental evidence that an existing crack will tend to close, if a new crack is formed in a rotated direction.

5 TEST BEAMS

A number of test programs have been carried out for the verification of the developed flexure-shear interaction design model [4,5]. The three test beams shown in Fig. 5 are used to validate the developed finite element model described in this paper. The variations in the test beams included the shear span to depth ration a/d (1.75 for Beam type A2 and 4 for Beam types C1.8 and C1.8(T)), the longitudinal reinforcement ratio ρ (2% for Beam type A2 and 1.8% for Beam types C1.8 and C1.8(T), the beam cross section and the detailing of the stirrups based on proposed (A2 and C1.8) and traditional approaches (C1.8(T)). Beam type A2 having a/d = 1.75 was used to validate the proposed model for type III (short) beams that lie to the left of the lowest point (a/d =2.5) in Kani's valley[1]. It should be noted that the detailing of stirrups for this beam based on the proposed approach is similar to traditional detailing except that in this beams the stirrups were extended inside the middle span to a distance equal to half the beam depth to prevent crushing of compression concrete adjacent to loading pint reported to occur in type III beams[1]. Two beam types C1.8 and C1.8(T) with a/d = 4 were used to validate the proposed model for type II (long) beams that lie to the right of the lowest point in Kani's valley. The traditionally detailed beam type C1.8(T) was included for comparison purposes. Beam type C1.8 was identical to beam type C1.8(T) except that it was detailed using the proposed model.

6 MATERIALS AND TESTING

For comparison purposes, the quality and characteristics of the concrete constituent materials remained consistent throughout the test program. Ordinary Portland cement and uncrushed aggregates were used throughout the investigation. The aggregates were well graded and free from any impurities, which might have adversely affected the bond between the aggregates and the cement paste. The coarse aggregates had a maximum size of 20 mm. High tensile strength deformed bars with nominal diameters (Φ) of 20 (A_s = 310.4 mm^2 and f_y = 500 MPa) and 25 mm (A_s = 483.9 mm^2 and f_y = 526 MPa) were used for the longitudinal reinforcement. Plain round mild steel bars with nominal diameters (Φ) of 8 (A_s = 49.9 mm^2 and f_y = 421 MPa) and 10 mm (A_s = 78 mm^2 and f_y = 441 MPa) were used for the stirrups and the secondary reinforcement. The steel bars were cleaned to remove surface rust in order not to weaken the bond with the concrete. To prevent anchorage failure of the longitudinal steel bars, the beams were extended 300 mm beyond the supports as shown in Fig. 5.

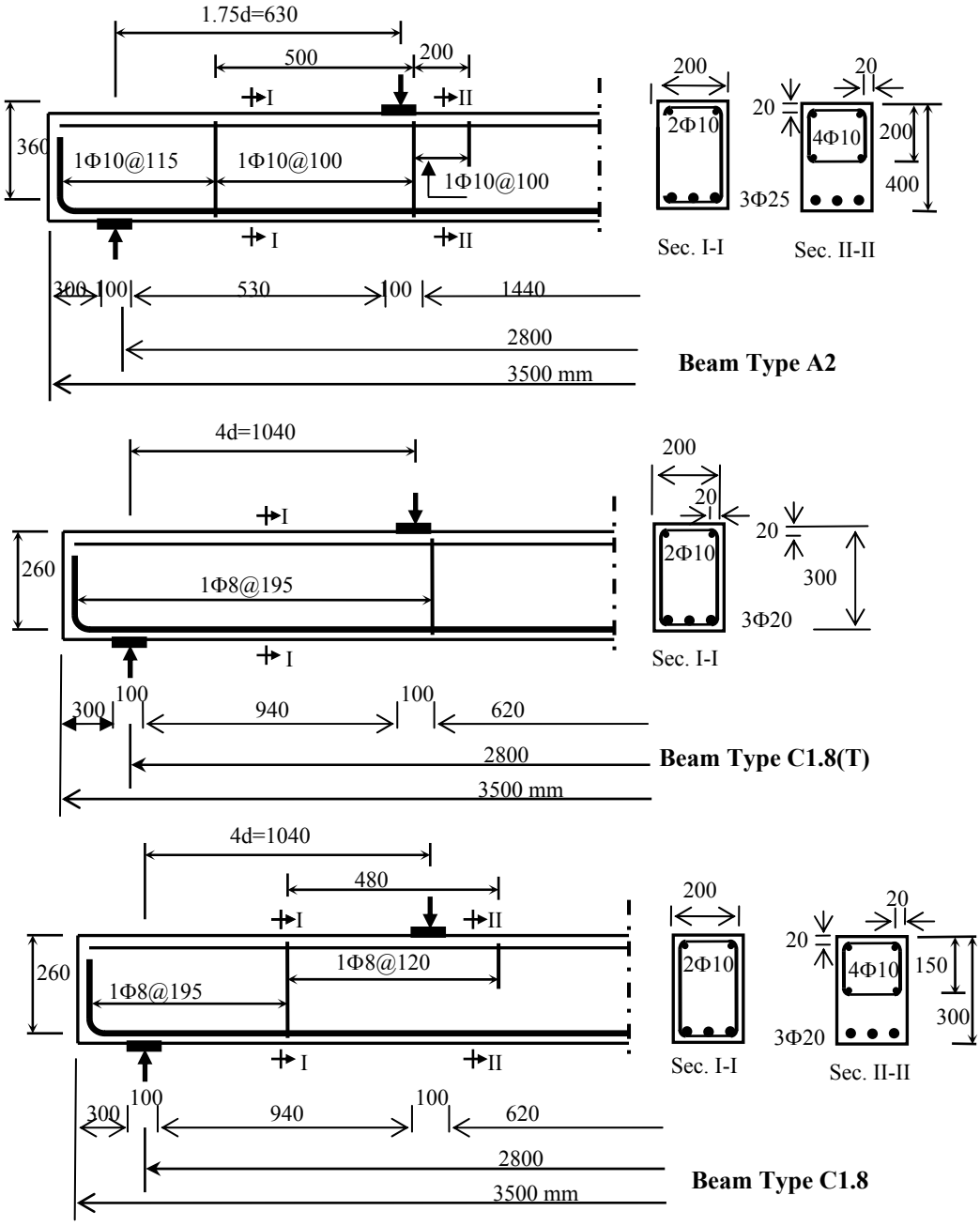

Fig. 5 Details of test beams.

The beams were cast in shutters made from structural steel channel sections. The beams and the control cylindrical specimens were cast and stored in their molds inside the laboratory under ambient conditions. They were normally covered with damp hessian over which polythene sheeting was tightly wrapped. The beams were removed from the shutters before testing and whitewashed to enable the early identification of cracks under loading. A grid consisting of horizontal and vertical lines was drawn on the surface of each beam to act as a reference for the cracks. The beams were loaded using a servo-controlled universal test machine with the four point loading arrangement shown in Fig. 1. The load was distributed from the test machine to the test beams using a structural steel spreader beam. A hinge, designed to ensure that the load was centrally

applied and to permit rotation of the spreader beam was used at the connection point between the test machine and the spreader beam. The beams were supported at one end on an assembly consisting of a roller and sandwiched between two steel plates. At the other end a rocker arrangement was used to prevent accidental lateral movement of the beams, however, the bearing plate was free to rotate during testing. The beams were tested under displacement control at a predetermined rate of 2 mm/minute. After each load increment, the beams were inspected for cracks. A crack width microscope with a resolution of 0.02 mm was used in the investigation. The cracks were marked on each face of the test beams at various loading levels. Linear Variable Differential Transducers were used to measure the deflection at the supports, the loading points, and at the mid-span of each beam. The displacement transducers were mounted on an independently supported frame and connected to a series of general purpose electronic indicators. The resolution of the indicators was approximately 0.01 mm.

7 FINITE ELEMENT ANALSIS OF TEST BEAMS

The beams A2, C1.8 and C1.8(T) were analyzed using a finite element computer program [13] after accounting for the aforementioned material modifications. Taking advantage of symmetry, only one half of the beam was considered. The beams were modeled using two modeling concepts of reinforcement shown in Fig. 6. One using discrete model for both the main and the secondary reinforcement, and the second using mixed model. The main reinforcement (longitudinal bars) were modeled as a discrete one dimensional truss element and the secondary reinforcement (stirrups) were modeled using smeared model. Fig. 7 shows the two model concepts for beam C1.8 and Table 1 summarizes the material properties of the analyzed beams. Unfortunately, actual measurement of concrete modulus of elasticity was not available. Therefore the ACI [1] and EC2 [16] corresponding formulas were used, which resulted in E_c ranging from 20000 to 24000 MPa. The concrete tensile strength was assumed to range from 2 to 3 MPa of the concrete compressive strength. The energy convergence criterion was used where the iteration tolerance for all meshes was 0.1% up to about half of the beam loading capacity and 0.01 % until the failure load.

Table 1. The material used in analysis.

Property	E_c (MPa)	f_c (MPa)	f_t (MPa)	ε_c	ε_{cu}	E_s (MPa)	E_H (MPa)	f_y (MPa)
Beam A2	2200	26	3.0	variable	variable	200000	2000	441-526
Beam C1.8	variable	27	variable	variable	variable	200000	2000	421-500
Beam C1.8(T)	2200	27	3.0	0.0023	0.003	200000	2000	421-500

8 RESULTS FROM TESTS AND FINITE ELEMENT ANALYSIS

Table 2 includes the measured concrete strength f_c' and summarizes the theoretical "M_t", actual "M_f" and finite element analysis "M_{FEA}" flexural capacities for the test beams. In order to evaluate the serviceability requirements the diagonal and flexural crack widths, and the mid-span deflections at working load, at ultimate capacity, and just before unloading are given in Table 3. Fig. 8 shows the load-mid span deflection curves. The deflected shape of the test beam C1.8, the crack pattern and the flexure stress distribution are shown in Figs. 9, 10 and 11, respectively.

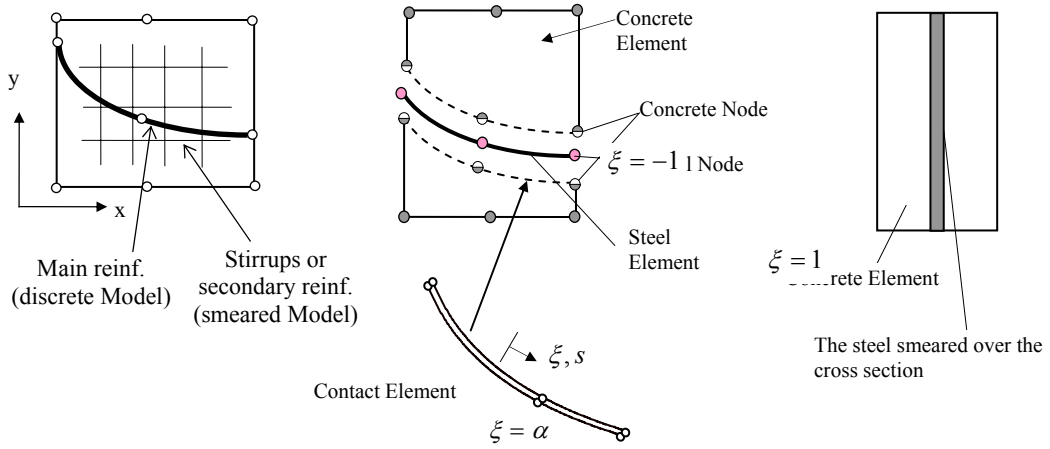

Fig. 6 Discrete and smeared model of steel reinforcement.

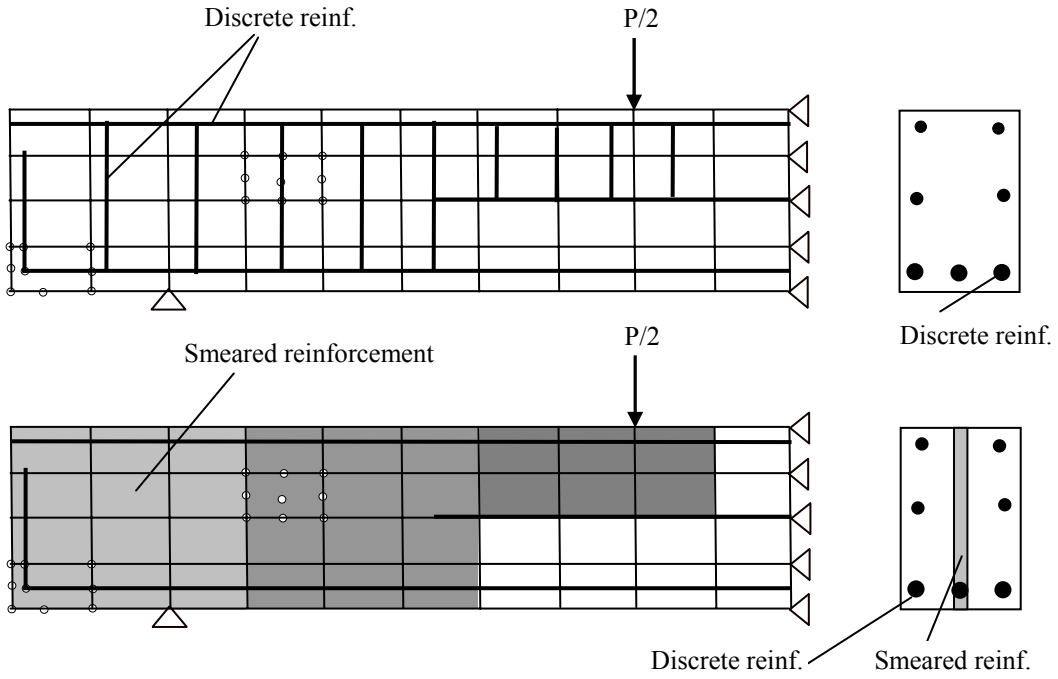

Fig. 7 F.E. Modelling of Beam C1.8: (a) Discrete and (b) Mixed reinforcement Models.

Table 2 Test and analytical results.

Beam Type	a/d	p %	f_c' MPa	Flexural capacity, kN.m			M_f/M_t
				Measured (M_f)	Theoretical (M_t)	Analytical M_{FEA}	
A2	1.75	2.0	26	252.2	218.6	251	1.15
C1.8	4.0	1.8	27	105.7	101.8	113	1.04
C1.8(T)	4.0	1.8	27	110.0	101.8	115	1.08

The test results have shown that all of the test beams reached their full flexure capacities and eventually failed in flexure by spalling of the concrete compression zone in the

regions of the beams subjected to maximum bending moments. Thus, the shear failure was prevented in all beams including those designed and detailed based on the flexure-shear interaction model. In beam type A2 diagonal cracks developed in the shear spans as an extension of existing flexure cracks. The diagonal cracks extended towards the loading points and were arrested by the confining influence of the stirrups in the concrete compression region. The flexure and the diagonal cracks proliferated and widened with increasing load. After reaching ultimate load, spalling of the concrete cover was noted in this beam. The beam eventually failed by spalling of the compression concrete and widening of the flexural cracks in the mid-span region. This obtained flexural behavior agreed with the FE analysis. Fig. 8 shows the load deflection curve from finite element analysis for Beam A2, compared with the experimental values. The stiffer behavior of the finite element analysis can be reduced by using a small modulus of elasticity as will be discussed in analysis of beam C1.8 and C1.8(T). From the FE results there is no significant difference between using the discrete or mixed finite element model.

In type C beams the traditionally detailed beam type C1.8(T) failed in a typical flexural failure mode. The flexural and diagonal cracks developed and widened under increasing loads. The diagonal cracks developed after the flexural cracks and were generally wider than the flexural cracks up to the ultimate load. Beam type C1.8 detailed using the flexure-shear interaction model also failed in a typical flexural failure mode as shown in Figs. 8 and 11. The FE analysis showed almost identical behaviors of beam types C1.8 and C1.8(T). Fig. 8 shows the effect of the modulus of elasticity in the analysis of beam C1.8. An increase in the modulus of elasticity increases the structure stiffness. The same figure shows also the load displacement curve compared with the experimental values for Beam C1.8 using the discrete and mixed model with different modulus of elasticity. The two models show almost the same results. Fig. 9 shows the deflected shape of beam C1.8 near the ultimate load.

The crack pattern and propagation of the beam C1.8 under load of 100 kN and 180 kN are shown in Fig. 10. It can be seen that some of the diagonal cracks have developed after the flexural cracks. The crack pattern from test of beam C1.8 is shown in Fig. 11 for comparison purposes. The two crack patterns were similar in the two cases. The normal flexural stresses in Fig. 12 for beam C1.8 indicate that some of the concrete elements have reached their full flexural strength.

With regards to load carrying capacity and ductility, all of the test beams reached their full flexural capacity as can be noted from Table 2. The ratio M_f/M_t ranged from 1.04 (beam type C1.8 to 1.15 (beam type A2). The ductility of test beams was related to their ability to undergo a significant deflection in the post-elastic range without a substantial reduction in its strength. The measured mid-span deflections for the test beams shown in Fig. 8 and Table 3 indicated that all beams behaved in a typical ductile manner. The ductility obtained from the test beams ranged from 38mm (beam type A2) to 50mm (beam type C1.8(T)). The test results in Fig. 8 and Tables 2 and 3 confirmed the similarity in the behavior of beam types C1.8 detailed using the flexure-shear interaction model and the traditional beam C1.8(T). The stiffness, the ductility and the load carrying capacity M_f/M_t obtained from the two beam types were almost identical.

The requirements of the serviceability limit state with respect to deflection and flexural crack widths at service load levels, are normally satisfied by following straightforward

procedures in which the maximum deflection and flexural crack widths are assigned limiting values [1,2].

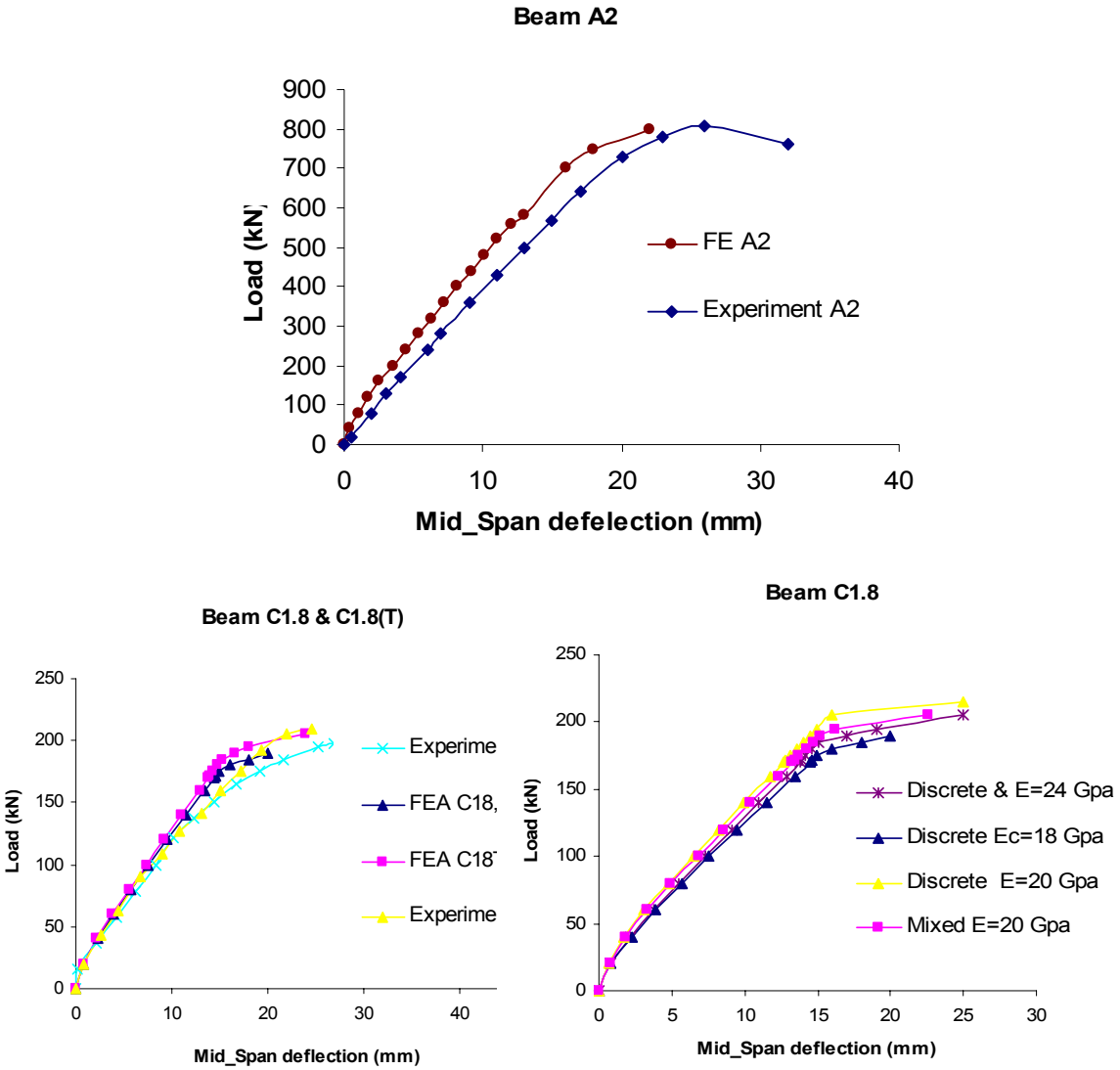

Fig. 8 Mid-span load deflection curves.

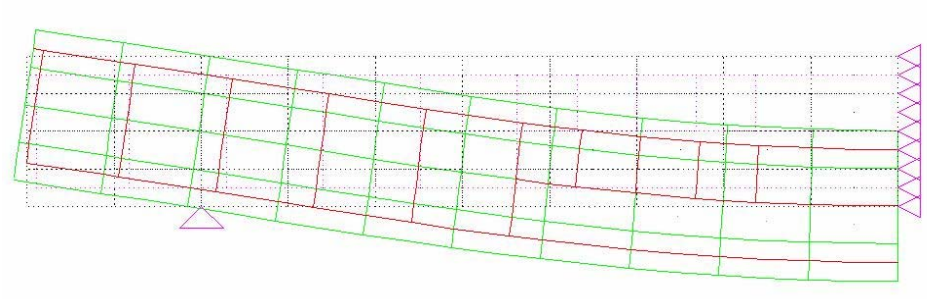

Fig. 9 Deflected shape of beam C1.8 near the ultimate load.

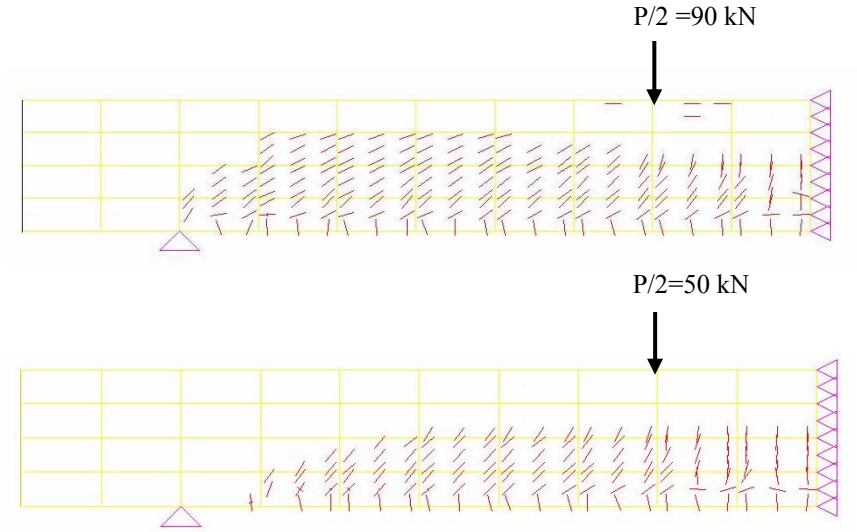

Fig. 10 Cracks propagation of under increased loading of Beam C1.8.

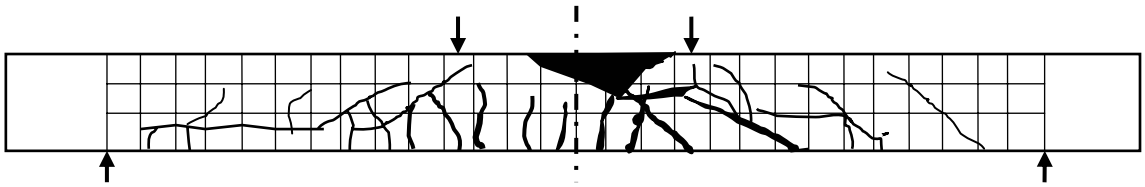

Fig.11 Crack pattern of beam C1.8.

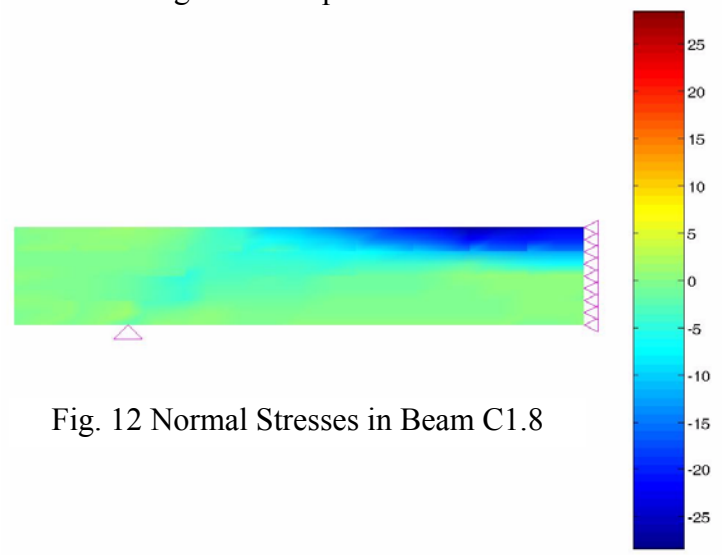

Fig. 12 Normal Stresses in Beam C1.8

Table 3 Crack width and deflection measurements.

Beam type	At working load leve				At ultimate load level				Before unloading			
	Load	Defl.	Crack width, mm		Load	Defl.	Crack width, mm		Load	Defl.	Crack width, mm	
	kN	mm	Flex.	Diag.	kN	mm	Flex.	Diag.	kN	Mm	Flex.	Diag.
A2	484	12	0.35	0.45	806.1	25	1.0	1.4	174	38	15	1.4
C1.8	121	12	0.3	0.3	201.8	36	2.5	3.0	25	39	4.0	6.0
C1.8(T	126	11	0.3	0.2	210.0	26	0.7	0.9	135	50	6.0	1.2

The flexural crack width should not exceed 0.3mm and the final deflection should not exceed either the span/250 based on the requirements of BS8110. The corresponding

values in the ACI Code of Practice are 0.41mm and span/360 (live load deflection) respectively. In the case of the test beams the allowable deflection under working load conditions, assuming that the long term deflection is included, would be approximately 11mm. In the case of the test beams the working load level was estimated, for comparison purposes, to be equal to 60% of the ultimate load. With regards to crack width, it is generally accepted that traditional design approaches result in diagonal crack widths, which satisfy the requirements of the serviceability limit state. The serviceability (deflection and crack width) obtained from beams detailed using the proposed model were compared with those obtained from traditionally detailed beams as shown in Table 3. In addition, the serviceability obtained from the beams was checked against the requirements of the serviceability limit state. The deflection at working load levels measured for the test beams just satisfied the requirements of the serviceability limit state. Table 3 also shows that the flexural crack widths at working load levels obtained from all of the beams were in the order of 0.3mm. The measured crack widths satisfy the serviceability limit state requirements (0.3mm or 0.41mm based on the requirements of either the BS8110 or ACI Codes of Practice respectively). The diagonal crack widths at working load levels obtained from all of the test beams did not exceed 0.4mm except for beam type A2 (0.45mm) which was designed based on the model however, its detailing was similar to traditional detailing.

9 CONCLUSIONS

1. The non-linear finite element model that accounted for the enhancement effects of confining stirrups succeeded in predicting the structural behavior of the test beams including those detailed based on the flexure-shear interaction model.
2. The smeared modeling of the stirrups showed same results as the discrete model.
3. There were good agreements in the load deflection curves between the results obtained from the tests and finite element analysis.
4. The crack patterns were almost the same for both the test beams and the analytical results which both indicated a flexural failure mode.
5. It is recommended to study the influence of the bond behavior between concrete and steel using the contact element.
6. Beam types A2 and C1.8 detailed based on the proposed flexure-shear interaction design model failed in flexure after reaching their full flexural capacity. Therefore, with respect to the ultimate limit design state, the proposed model has been validated experimentally for normal-size beams made from normal-strength concrete.
7. The serviceability (deflection and crack widths at service load levels) of the beams detailed using the proposed model and the traditional beam was found, in general, to satisfy the serviceability limit state design requirements.
8. The ductility of the beams designed using the flexure-shear model was similar to that found in the traditional beams.

REFERENCES

1. ACI Committee318,“Building Code Requirements for Reinforced Concrete (ACI 318-02) and Commentary (ACI 318R-02),” American Concrete Institute, Detroit, 2002, 443 pp.

2. British Standard Institution. BS 8110, "Structural Use of Concrete, Part 1, Code of practice for design and construction," 1997, 128 pp.
3. Mörsh, E., "Der Eisenbetonbau," 3rd ed., published in English as "Concrete-Steel Construction," New York, Engineering News Publishing Co., 1909.
4. Ziara, M. M., Haldane, D. and Kuttab, A. S., "Prevention of Diagonal Tension Failures in Beams Using a Flexural-Shear Interaction Approach," Magazine of Concrete Research (London), Vol. 51, No. 4, August 1999, pp 279-293.
5. Ziara, M. M. and Haldane, D., "Flexure-Shear Model for Prevention of Diagonal Failures in Beams Made with High Strength Concrete," The Eighth East Asia-Pacific Conference on Structural Engineering and Construction: Challenges in the 21st Century, Singapore, *5-7 December 2001*.
6. Arafa, M. and MEHLHORN, G., "Direkt Erffasung der Vorspannung mit nichtlinearer FE-Berechnung", (in German), *Bautechnik,* (Germany) 78 (2001), Heft 10. pp 724-732, in German
7. El-Mezaini, N. and Citipitoglu, E., "Finite Element Analysis of Prestressed and Reinforced Concrete Structures" Journal of Structural Engineering, Vol. 117, No. 10, October 1991.
8. Keuser, M., "Verbundmodelle für nichtlineare Finite–Elemente–Berechnungen von Stahlbetonkonstruktionen," Dissertation, Technische Hochschule Darmstadt, VDI Verlag, Düsseldorf, 1985
9. Figueiras, J.A., "Ultimate Loads Analysis of Anisotropic and Reinforced Concrete Plates and Shells," Ph.D. Thesis, Department of Civil Engineering, University of Wales, UK, September, 1983.
10. Dinges, D.,"Vergleichende Untersuchungen von Stahlbetonflächentragwerken unter Berücksichtigung physikalischer und geometrischer Nichtlinearitäten," Dissertation D17, Technische Hochschule Darmstadt, 1987
11. Kollegger, J., "Ein Materialmodell für die Berechnung von Stahlbetonflächentragwerken," Dissertation, Universität Gesamthochschule Kassel, 1988.
12. Sheikh S. and Yeh C.,"Analytical moment curvature relations for tied concrete columns," Journal of structural Engineering, ASCE 1992, Vol 118 No. 2 February, p.p 529-544.
13. Segnid, "Finite Element Computer Program for Geometrical Physical Nonlinear Analysis," User Manual (Editors. SCHULZ, J. und STRIPPEL, R., ARAFA, M.) Version 3.20, Fachgebiet Massivbau, Universität Gesamthochschule Kassel 1996.
14. Hofstetter, G. and Mang, H. "Computational Mechanics of Reinforced Concrete Structures," Friedr. Vieweg & Sohn , Braunschweig/Wiesbaden, 1995.
15. Ngo, D. and Scordelis, A. C.,"Finite Element Analysis of Reinforced Concrete Beams," ACI Journal, Vol. 65 , pp. 757-766, 1967.
16. Eurocode 2, Teil I, "Planung von Stahlbeton- und Spannbetontragwerken," Beuth Verlag GmbH, Berlin, Juni 1992.